Tree Stem Diameter Estimation from Terrestrial Point Clouds

Mona Forsman
Faculty of Forest Sciences
Department of Forest Resource Management
Umeå

Doctoral thesis
Swedish University of Agricultural Sciences
Umeå 2018

Acta Universitatis agriculturae Sueciae
2018:54

Cover: Intensity image of a terrestrial laser point cloud of a spruce forest.

ISSN 1652-6880
ISBN (print version) 978-91-7760-248-4
ISBN (electronic version) 978-91-7760-249-1

Print: SLU Service/Repro, Uppsala 2018

Tree Stem Diameter Estimation from Terrestrial Point Clouds

Abstract

Forest owners, governments, and environmental organizations demand forest information for planning of forest operations, estimation of value, and for environmental monitoring. This information is collected using airborne and satellite remote sensing combined with field inventory of sample plots.

Stem diameter is measured with calipers, which is labor-intensive. Terrestrial sensors could make the inventory faster, and more samples could be taken. Sensors mounted on forest harvesters could produce maps of the trees left after forest operations, or collect data for an operator support system.

The first article describes a photogrammetric method using a multi-camera rig for estimation of stem diameter and position on field plots. Problematic light conditions reduced the usable amount of field plots. On adequate field plots, 76% of the trees were detected and positioned, and on 40% of the trees the diameters could be estimated. In the second article, the results from a mobile laser scanning project was improved by treating the data line-wise, and by using the intensity of the laser points as a quality value. The RMSE of the stem diameters was reduced from 24% to 14%, but the bias increased slightly from -1.9% to 2.3%. The edge points on the stems were identified as an error source since they were not found along the expected circle. The third article investigates this edge point problem by simulation of laser scanner/tree combinations. A relationship between the diameter error and the footprint size relative to the stem diameter was found. Commonly used mobile laser scanners were concluded to give a relative bias of 10% or more when estimating diameters using circle fit methods. In the fourth article, a panorama image of the intensities of a laser scanner point cloud was used to detect trees, with adequate results.

The overall conclusions are that point clouds from the various sensors are useful for estimation of tree diameter and positions, but they have sensor-dependent properties that can introduce errors. These properties, and the precision requirement should be considered when the data acquisition is planned and the sensor is selected.

Keywords: Forest inventory, Point cloud processing, Mobile mapping, Precision forestry, Mobile laser scanning, Simulation, Terrestrial laser scanning, Tree stem diameter, Terrestrial photogrammetry, Error analysis

Author's address: Mona Forsman, SLU, Department of Forest Resource Management, Skogsmarksgränd, SE-901 83 Umeå, Sweden

Tree Stem Diameter Estimation from Terrestrial Point Clouds

Sammanfattning

Skogsägare, myndigheter och miljöorganisationer behöver skoglig information för planering av skogsskötsel, värdering och miljöövervakning. Informationen samlas in med en kombination av flyg- och satellitfjärranalys och stickprovsinventeringar av provytor i fält.

Stamdiameter mäts med klavar, vilket är arbetsintensivt. Markbaserade sensorer skulle kunna göra inventeringen snabbare, och fler stickprov skulle kunna inventeras. Sensorer på skördare skulle kunna leverera trädkartor över vad som är kvarlämnat efter en avverkning, eller de skulle kunna samla in data till ett förarstödsystem.

Den första artikeln beskriver en fotogrammetrisk metod för skattning av stamdiameter och position på provytor. Problematiska ljusförhållanden minskade mängden användbara provytor. På de användbara provytorna positionerades 76 % av träden och för 40 % kunde diametrarna uppskattas. I den andra artikeln förbättrades resultaten från ett mobilt laserskanningsprojekt genom att behandla punktmolnet linjevis, och genom att använda punkternas intensitet som ett kvalitetsvärde. Stamdiameterskattningens RMSE reducerades från 24% till 14%, men biaset ökade något från -1.9% till 2.3%. Kantpunkterna på stammarna identifierades som en felkälla eftersom de inte hittades längs den förväntade cirkeln. Den tredje artikeln undersöker detta kantpunktsproblem genom simulering av laserskanner / trädkombinationer. En relation mellan diameterfelet och laserns träffyta i förhållande till stamdiametern hittades. Vanligt använda mobila laserscannrar visade sig ge en relativ bias på 10 % eller mer i skogliga tillämpningar. I den fjärde artikeln användes en panoramabild av intensiteten hos ett laserpunktmoln för att upptäcka träd med lyckat resultat.

Slutsatserna är att punktmoln från de olika sensorerna är användbara för uppskattning av träddiametrar och positioner, men de har sensorberoende egenskaper som kan införa fel. Dessa egenskaper och precisionskravet bör beaktas när datainsamlingen planeras och sensorn väljs.

Nyckelord: Skogsinventering, Punktmolnsbehandling, Mobil kartläggning, Precisionsskogsbruk, Mobil laserskanning, Simulering, Markbaserad laserskanning, Trädstamsdiameter, Markbaserad fotogrammetri, Felanalys

Author's address: Mona Forsman, SLU, Institutionen för skoglig resurshushållning, Skogsmarksgränd, 901 83 Umeå, Sverige

Dedication

Till Tomas, Sixten och Olivia

Contents

List of publications

This thesis is based on the work contained in the following papers, referred to by Roman numerals in the text:

I Forsman, M.*, Börlin, N. and Holmgren, J. (2016). Estimation of Tree Stem Attributes Using Terrestrial Photogrammetry with a Camera Rig. *Forests*, 7(3), 61.

II Forsman, M.*, Olofsson, K., Holmgren, J. (2016). Tree Stem Diameter Estimation from Mobile Laser Scanning Using Line-Wise Intensity-Based Clustering. *Forests*, 7(9), 206.

III Forsman, M.*, Börlin, N., Olofsson, K., Reese, H. and Holmgren, J. (2018). Bias of cylinder diameter estimation from ground-based laser scanners with different beam widths: A simulation study, *ISPRS Journal of Photogrammetry and Remote Sensing*, Volume 135, Pages 84-92.

IV Forsman, M. and Holmgren, J., Tree detection using intensity-based panorama images from terrestrial laser point clouds. (Manuscript)

Papers I-III are reproduced with the permission of the publishers.

* Corresponding author.

The contribution of Mona Forsman to the papers included in this thesis was as follows:

I Planned the study and field work with the co-authors. Carried out parts of the method development and programming. Carried out the data analysis. Wrote the major part of the manuscript with input from the co-authors.

II Developed the method and carried out the programming. Carried out the data analysis. Wrote the major part of the manuscript with input from the co-authors.

III Conceived the presented idea. Designed the major part of the simulation with input from the co-authors. Made the major part of the programming. Carried out the analysis. Wrote the major part of the manuscript with input from the co-authors.

IV Conceived the presented idea. Designed the method and carried out the programming. Carried out the analysis. Wrote the major part of the manuscript with input from the co-author.

Abbreviations

2D	Two-dimensional
3D	Three-dimensional
ALS	Airborne Laser Scanning
ATV	All-Terrain Vehicle
DBH	Diameter at Breast Height (1.3m)
GNSS	Global Navigation Satellite System
IMU	Inertial Measurement Unit
MLS	Mobile Laser Scanning
NFI	National Forest Inventory
PLS	Personal Laser Scanning
PS	Phase Shift
RANSAC	RANdom SAmple Consensus
RMSE	Root Mean Square Error
SfM	Structure from Motion
SGM	Semi-Global Matching
SIFT	Scale Invariant Feature Transform
SLAM	Simultaneous Localization And Mapping
TLS	Terrestrial Laser Scanner/Scanning
ToF	Time of Flight

1 Introduction

1.1 Forest information

Forest information has many purposes on different levels in the society. On a global level, changes in forest cover are monitored and estimations of carbon storage are done within the United Nation Framework Convention on Climate Change (UNFCCC). Many countries and regional authorities collect information for environmental reasons such as monitoring of land use, carbon storage, deforestation, wildlife, recreational reasons, as well as economic reasons (value of potential timber harvest). Forest owners use forest information for planning of management operations and harvest decisions (Wikström et al. 2011), however, uncertainty in forest information can lead to sub-optimal decisions (Duvemo & Lämås 2006). Forest height, tree species, stem diameter distribution, biomass, and wood volume are some of the interesting variables. After storms or wildfires, new data collection may be needed for assessing damages done to the forests. The new *precision forestry* paradigm (Holopainen et al. 2014) is stimulated by the new possibilities to automatically obtain detailed forest information, down to single tree level. The goal is to optimize forest operation using high resolution geographical information. Forest information is nowadays gathered using a combination of remote sensing and field measurements. Satellite images, airborne images, and airborne laser scanners are used for efficient coverage of large areas.

Remote sensing methods are operational for gathering of forest resource information, with interpretation of aerial photography for forest resources used in Sweden since the 1950s and satellite images since about the year 2000. Airborne laser scanning has been in use since 2002 in Norway. Photogrammetric point clouds are occasionally used. These operational methods measure the tree

crowns and not the stems. Tree height can be accurately measured using Airborne Laser Scanning (ALS; Næsset 2007). Information about the tree stems are needed for planning of forest operations to deliver material suitable to the industry's demands. Ground-based measurements are needed to make functions to improve the estimation of stem properties from the remotely measured tree crowns, and these methods need to be more efficient than the manual measurements used today.

Field inventory of sample plots is used for construction of models which link the remotely sensed variables to real forest variables. The field inventory is mostly done using calipers recording the diameter at breast height (DBH, diameter at 1.3 m above ground) (Fridman 2016). Sometimes the trees are measured twice, in perpendicular directions, and the mean value is used as the diameter. This reduces the error since the stem cross-section is usually slightly elliptical. Species for each tree are recorded manually. For determining tree positions (in cases where tree positions are of interest), ultrasonic trilateration might be used within the field plot. The plot can be globally positioned using high-precision Global Navigation Satellite System (GNSS). Wood volume can be calculated using the DBH measurement and the tree height from sample trees, using specific formulas (allometric equations) derived for different tree species (Näslund 1947). By connecting results from field measured sample plots and remote sensing data, one can make models for estimation of wood volume over larger areas with similar characteristics.

1.2 Terrestrial and mobile sensors in forestry

There are multiple purposes of ground-based sensors in forestry. In this thesis, a *terrestrial sensor* is a ground-based, stationary sensor. A *mobile sensor* is a moving sensor, either mounted on a vehicle (e.g., a car or a forest harvester), or a sensor carried by a person.

The main purpose of terrestrial, stationary sensors is to make forest inventory more efficient. Stationary terrestrial laser scanners (TLS) can scan a field plot in a couple of minutes. The diameter and the tree positions can be measured for trees visible to the scanner (Pfeifer et al. 2004; Olofsson et al. 2017; Liang et al. 2011; Maas et al. 2008). Additionally, TLS can be used for detailed studies of single trees, such as finding the stem diameter along the stem to determine the stem shape, or measuring branches to study trees growth, or to make detailed estimates of the wood volume in single trees (Hauglin et al. 2013, Hackenberg et al. 2015).

Terrestrial photogrammetry (i.e., measurements from images taken with ground-based cameras) has advantages in the form of lightweight equipment and additional information value from images that can be used for later manual interpretation by biologists/ecologists of ground coverage, habitats, and other data not traditionally collected. However, problems with occlusions can be significant in natural forests, as well as low image quality due to difficult illumination conditions under the forest canopy. Various approaches have been developed and tested, for example, using a hand-held single camera (Liang et al. 2014b), using a multi-camera rig (Forsman et al. 2012) and using cameras with stereoscopic fisheye lenses (Berveglieri et al. 2016).

Mobile sensors can, in the near future, be usable as a data collection device for extended operator support systems in forest harvesters (Liang et al. 2014a; Forsman et al. 2016; Ringdahl et al. 2013). Mobile laser scanners (MLS) can collect data about the forest along the driven track. Information about diameter and positions of trees around the harvester could be used for decision support during thinning to decide which trees to cut, and which ones to leave standing. A system that can extract the stem profile could provide recommendations on where to cut each stem to optimize the timber outtake. After thinning, an automatic report could be generated with information about the trees left in the forest, such as their positions, size and possibly also species.

Personal Laser Scanning systems (PLS; Liang et al. 2014d) are carried by a person and can collect data where the person carrying the device can walk. This kind of system may in the future be useful for inventory in areas sensitive to disturbance, as well as gaining information from larger parts of forest stands rather than just from sample plots.

1.3 Errors in forest measurements

All measurements include errors. The acceptable size of the errors depends on the intended use of the information. For monitoring of deforestation, for example, a classification of forest/non-forest can be enough, while a forest owner would not be happy if their actual outtake is half of the estimated stock. The Swedish Forest Map (“Skogliga grunddata”), the Forest Agency’s forest information service based on airborne laser scanning and National Forest Inventory (NFI) sample field plots, has an error of 17%–22% for wood volume, and 9%–13% for diameter at breast height when compared to field data for sample plots and stands (Nilsson et al. 2017).

Omission errors (missing an object) can happen, for example, when a forest field plot is laser scanned and some trees are occluded by other trees. The occluded trees will not be detected, and will be missing from the inventory. This

would result in a tree count that is too low, and estimations on stand level wood volumes would also be too low. Commission errors (false detection of an object that isn't there) may be the consequence if the point cloud processing method fails when shrubs, stones, or other objects are classified as trees. A method producing commission errors is not trustworthy, and would need manual guidance for better results. In manual inventory, an omission error would be, for example, a missed tree, and a commission error would be a tree recorded twice.

A future operator support system for forest harvesters could use high-precision diameter estimations both for selection of trees, and accurate bucking. For measuring full stem profiles, multiple accurate diameter measurements and their position along the stem are needed.

1.3.1 Quantification of errors

Measurement errors consist of two parts: a systematic part and a random part. The systematic error (for example, a measurement is always 10% too large) can be called bias, or offset depending on application and culture. The random part is called precision (for example, a measurement is sometimes smaller, sometimes larger). To quantify the random error, the variance of the residuals can be calculated.

In forest remote sensing, the root-mean-square error (RMSE) is often used to describe the accuracy, which is the combined measurement error. In this work we will follow the common nomenclature in forest remote sensing - using *bias* for the systematic error, and *RMSE* for the accuracy.

The bias calculation is shown in Eq. 1.

$$Bias = \frac{1}{N}\sum_{i=1}^{N}(\hat{d}_i - d_i) \tag{1.}$$

where N is the number of measurements, $\hat{d}_i$ is the estimated diameter of the i:th tree and d_i is the true diameter of tree i.

A bias can be dependent on the measurement setting, for example, the distance to the object. A high bias can be reduced/removed with calibration (as in model parameter fitting for empirical models), but should also be explainable.

RMSE is calculated as:

$$RMSE = \sqrt{\frac{\sum_{i=1}^{N}(\hat{d}_i - d_i)^2}{N}} \tag{2.}$$

where N is the number of measurements, $\widehat{d_i}$ is the estimated diameter of the i:th tree and d_i is the true diameter of tree i.

A high RMSE implies that the method has low repeatability, which could originate, for example, from unstable measurement methods, noise, or difficulties with segmentation of the object. A low RMSE relative to the measured quantity implies a method with good repeatability and high accuracy.

Errors from completely failed measurements are called *Gross errors*, or *Blunders*. These are not possible to handle statistically, and should usually be avoided by doing correct measurements. Gross errors can be handled as outliers, and be removed from the data set, however, it is bad practice to do that routinely. If gross errors are common, a better method should be developed. During a manual forest inventory, gross errors can occur as omission errors if a tree is missed during the inventory, or as commission errors if trees are accidentally measured twice. Another reported source of gross errors is malfunction of digital calipers. The errors of the DBH estimation will propagate through the equation for wood volume and give an error in the total estimates.

1.4 Photogrammetry

Photogrammetry is defined as the process of deriving metric information about an object through measurements made on photographs of the object (Mikhail et al. 2001). The term is mostly used to refer to the creation of 3D data (often point clouds) from images, but can also apply to measurements in images. With point correspondences between two or more images of the same object, knowledge about the cameras' internal geometry and the relative orientation of the cameras, 3D point clouds can be calculated.

1.4.1 The pin-hole camera

The pin-hole camera model describes how a 3D point $\boldsymbol{X}$ is projected onto a 2D point $\boldsymbol{x}$ in the image, see Figure 1. A 3-by-3 camera matrix K describes the internal geometry of the camera, and can be estimated by camera calibration.

If the coordinates of the 3D point $\boldsymbol{X}$ and the 2D point $\boldsymbol{x}$ are expressed in homogeneous coordinates and $\boldsymbol{X}$ is expressed with reference to the camera coordinate system, the projection $\boldsymbol{x}$ of $\boldsymbol{X}$ in the image plane may be computed as $\boldsymbol{x} = [\mathbf{K} \quad \mathbf{0}]\boldsymbol{X}$, where $\mathbf{0}$ is a 3-vector.

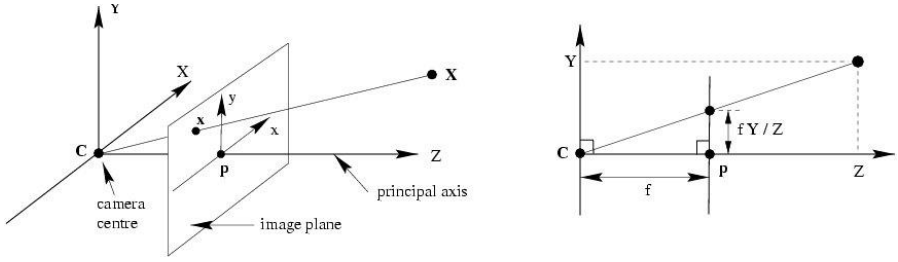

*Figure 1. The pin-hole camera model. A point **X** in 3D space is projected onto the point **x** on the image plane, at the intersection of the image plane and the line connecting **X** and the camera center **C**. The forward direction is in the Z direction, and is called the principal axis. The principal axis intersects the image plane at the principal point **P**, which is the optical center of the image. The focal length f is the distance between the image plane and the camera center, which is the focal point of the lens. In this image, the image plane is visualised in front of the camera center. In real cameras, the image plane is behind the center. Figure from: Multiple View Geometry, Hartley Zisserman (2000). Used with permission.*

The pin-hole camera model is straight-line-preserving, i.e., straight lines in the world are imaged as straight lines in the image. The aperture in the pinhole camera is infinitely small. The aperture in a real camera has a finite size. To obtain a sharp image, lenses are introduced to bend the incoming rays of light. A side effect of having a lens is lens distortion, which has the implication that images of straight lines are curved. In images taken with wide-angle objectives this phenomenon is obvious, and tree stems, for example, will be visually curved. This form of distortion is called *barrel distortion* (Figure 2). The effect of lens distortion can be modelled by polynomials (Brown 1971). The coefficients of the polynomials can be estimated in a process called camera calibration. The lens distortion coefficients can be used to correct the measured image coordinates and/or rectify the image.

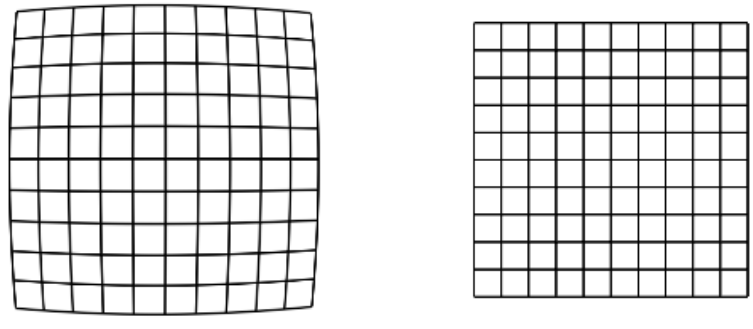

Figure 2. A barrel-distorted square grid (left) and the rectified image (right).

1.4.2 Relative orientation

The relative orientation, the position (x,y,z) and direction (yaw ψ, pitch θ, roll φ) of a camera relative to another camera, is required for calculation of 3D coordinates. A matrix R and a translation vector C then translates the 3D coordinates from the coordinate system centered in camera 1 to the coordinate system of camera 2, which can be constructed from the orientation parameters (Figure 3).

When a projection is calculated in a camera that is not centered in the origin of the world coordinate system, the relative orientation has to be incorporated in the camera matrix, such that
$P = KR[\boldsymbol{I}| - \boldsymbol{C}]$, where P is the projection matrix, K is the camera matrix, R is the relative orientation, I is the identity matrix, and C is the coordinates for the camera center (in matrix notation). For further information about the rotation matrix, see for example Strang (2003) or Angel (2009). The relative orientation between a pair of images can either be estimated using features in each image pair (*single-camera photogrammetry*), or by using cameras mounted on a rig with fixed geometry (*camera rig*).

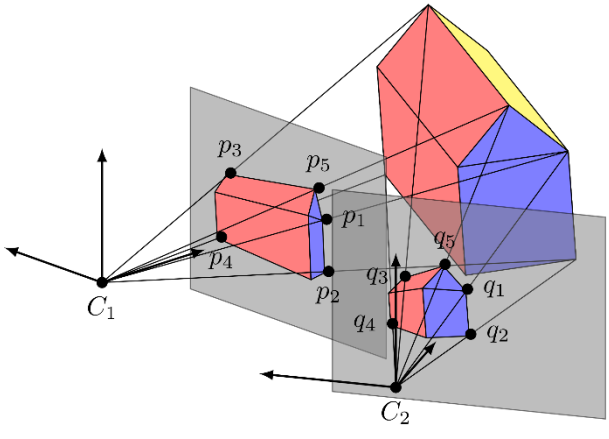

Figure 3. Two views of the same object. Each camera has its own coordinate system with the origin in the camera center. A transformation matrix R with the translation and rotation needed to transform the 3D coordinates relative to camera C_2 into camera C_1's coordinate system. Image source: Niclas Börlin, with permission.

1.4.3 Epipolar geometry

The relationship between two images of the same object taken from different points of view is described by the epipolar geometry of the images. The two centers of the cameras, C_1 and C_2 , spans the baseline (see Figure 4). The epipoles, e_1 and e_2, of each camera is the projection of the other camera center

on the image plane of each camera. Every plane determined by an arbitrary point Q and the baseline between C_1 and C_2 is an epipolar plane. The line of intersection of the image plane and the epipolar plane is called the epipolar line. When the projection point q_1 of a point Q is known in image 1, the projection point q_2 is restricted to lie on a line through the projection of the camera center C_1 and the point q_2 in the image plane of the second camera. This line intersects the epipole e_2.

The algebraic representation of the epipolar geometry is the fundamental matrix F, which is defined by the relation $q_1^T F q_2 = 0$. The fundamental matrix can be found using multiple point correspondences in the images. See the 7-point or 8-point algorithms found in Hartley and Zisserman (2003).

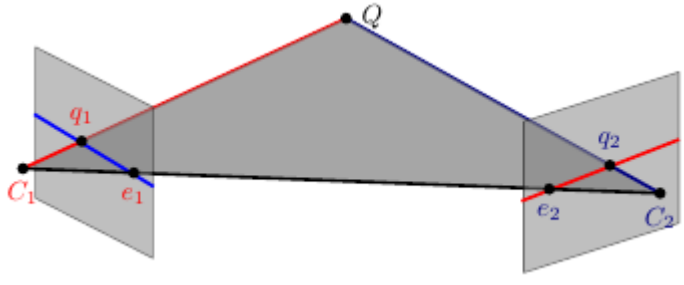

Figure 4. The epipoles e_1 and e_2 are the projection of the other camera's center, C_2 and C_1 on the respective camera's image plane. The epipolar plane for a point Q is spanned by the point Q and the camera centers C_1 and C_2. The epipolar lines are the intersection of the epipolar plane and each camera's image plane. The projections of the point Q are constrained to lie on the respective epipolar lines. Image source: Niclas Börlin, with permission.

1.4.4 Forward intersection

In the ideal case, the position of the 3D point can be calculated as the intersection of two 3D rays. Each ray passes through the corresponding image point and the optical center of the camera. This point could be calculated by solving the equation system in Eq. 3.

$$\begin{aligned} \boldsymbol{x} &= P\boldsymbol{X} \\ \boldsymbol{x}' &= P'\boldsymbol{X} \end{aligned} \qquad (3.)$$

where $\mathbf{x}$ and $\mathbf{x}'$ are the homogenous coordinates for the matched points, P and P' are the respective projection matrices and $\boldsymbol{X}$ is the calculated 3D point.

However, if there are any errors in the coordinates for the points, or in the camera parameters, the lines will not intersect. Hence, in practice an approximate point has to be calculated. This process is known as forward intersection.

1.4.5 Feature matching

In this work, feature based matching with epipolar constraint is used in combination with forward intersection for calculation of 3D points. The method used in this work, Scale-Invariant Feature Transform (SIFT, Lowe 2004), detects distinct features in the images, which are then matched to the most similar feature in the other image. To reduce the amount of comparisons, and to lower the risk of false matches, the matching can be constrained, for example, by the epipolar geometry. The point coordinates are then used for calculation of the 3D point cloud using forward intersection, as described earlier.

1.4.6 Other approaches

Another approach to create 3D data from images is pixel-wise matching, for example, Semi-Global Matching (SGM, Hirshmüller 2008). SGM searches pixel-wise correspondences in a pair of images, and uses the disparity for 3D calculation. This approach is suitable for images with large overlaps. Structure from Motion (SfM, Hartley & Zisserman 2003, Westoby et al. 2012) is a method from computer vision that is gaining popularity for photogrammetry. SfM follows features such as points and lines detected in images from a moving camera, and uses the features to calculate camera position and the structure of the detected features.

1.4.7 Error sources in photogrammetry

There are many possible error sources that can affect the quality of a photogrammetric point cloud. Dai et al. (2014) have analysed the topic in depth.

The error sources can be organized as

- Errors in the estimation of the internal camera parameters (e.g., type, principal point, principal distance, and camera lens distortion coefficients).
- Errors in the estimation of the external parameters (relative camera position and orientation).
- Errors in feature extraction and matching
  - Small errors - precision of coordinates.
  - Gross errors - point from a false matching of features.
- Occlusions in the view that leads to a point cloud lacking points in certain areas.
- Instability in the hardware.

All the possible errors will propagate through the forward intersection and give higher errors in the calculated points.

The planning of the image acquisition is critical to obtain a point cloud of high quality. A wide baseline between the cameras gives a better geometry for the calculation of the 3D points, but will also make the feature matching more difficult with different perspectives from different angles of incidence, which can increase the errors in the feature coordinate and the risk of false matches. A wide baseline will give smaller overlaps, and smaller parts of the images that can be used for the matching.

A shorter distance to the object captures more details, and a larger amount of points can be matched. A short distance will also give higher accuracy than longer distances. The camera hardware should have as small lens distortion as possible and a light-sensitive, high-resolution sensor. A large number of images gives a higher potential to finding matched points, and a denser point cloud, but will also take longer time to capture on site, and longer time to process.

The attainable precision of a photogrammetric point cloud differs for different object setups. For a small object in an indoor studio with good lighting and controlled camera positions, a higher precision is possible than for outdoor objects in only natural light, with larger distances, occlusions and handheld cameras.

1.5 Laser scanning

A laser scanner determines the distance to a reflecting object by measuring the time a pulse of laser light takes to reach the object and return to the scanner (Baltsavias 1999). There are two different kinds of laser scanners: Time-of-Flight (ToF) “pulse laser”, and Phase Shift (PS) “continuous wave”, which each work according to different principles. In this work, we focus on ToF laser scanners.

1.5.1 Principle

A ToF scanner measures the time for a laser pulse emitted by the laser scanner to reach a target and return to a sensor on the scanner (Figure 5). A distinctive pulse of laser light is emitted from the laser scanner and is reflected by the target, and a part of the pulse returns to the laser scanner. The total time *t* for the pulse to travel from the scanner, to the object and back to the scanner is measured. The distance *d* between the scanner and the object is calculated from the measured time *t* by $d = c \cdot t/2$, where c is the speed of light.

1.5.2 The laser pulse

The spatial shape of the laser pulse is a cone with its tip at the laser scanner, and the cone is often called the laser beam. The pulse is commonly in the order of a meter long, which corresponds to a time of 3 ns at the speed of light. The angular width of the cone is called the beam width, and the area illuminated by the beam on an object is called the footprint. Objects within the cone (and within the working distance) will give echoes. Ideally, the temporal shape of the laser pulse should be a square pulse, with vertical flanks and a constant intensity. In reality, for technical reasons, the pulse shape is more complex, often with an intensity spike in the beginning of the pulse and then descending intensity.

1.5.3 Echo detection

The returning echo signal will have a much lower amplitude than the emitted pulse, since only a small fraction is reflected back to the scanner and received by the detector. There are different methods in use for echo detection. The exact timing of the echo detection depends on the shape of the echo and the echo detection method. The shape of the returning signal will be affected by the target geometry, for example, a target that is sloped within the footprint area will prolong the echo with a less steep leading flank than the original pulse had. Common detection methods are either based on intensity thresholds, leading edge slopes, constant fraction of amplitude, or intensity maxima (Jutzi & Stilla, 2003, Wagner et al., 2004, Shan & Toth, 2009).

1.5.4 Angular resolution

Between the centers of adjacent beams there is an angular separation or angular resolution, which may differ in the horizontal and the polar direction. In many scanners the angular separation is smaller than the beam divergence angle, resulting in overlapping beams and no risk of missing objects between the beams. The angular resolution determines how dense the measurements will be, and hence the point cloud density and the amount of points reflected by each object.

1.5.5 Multiple echoes

A pulse can be partly reflected by multiple objects, and the echo signal might have multiple local maxima in the signal. If the angle of incidence at the target is not perpendicular, the footprint will be smeared out, resulting in a distorted echo with a slanted leading edge. As a result, the returning echo signal can have

a complex shape. Most modern laser scanners can detect and record multiple echoes per pulse. Some scanners record the whole echo, giving a signal that can be used for further processing.

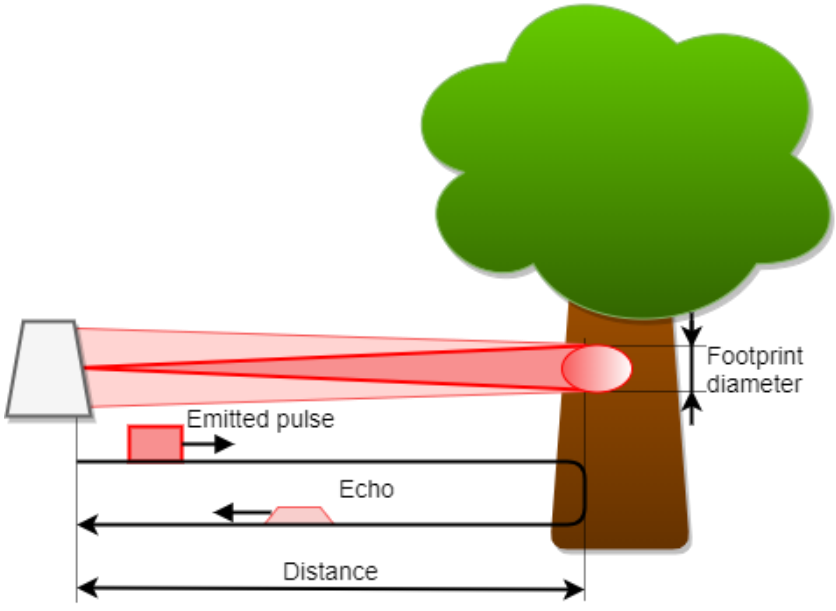

Figure 5. Principle of a laser scanner. A square pulse is emitted from the laser scanner and is reflected by the target, here a tree.

1.5.6 Error sources in laser scanning

Laser measurements are often regarded as very precise measurements. Noise levels of less than one millimeter in combination with systematic errors of less than two millimeters at 100 m distance are claimed in data sheets for TLS equipment. However, this claim requires certain conditions, such as that the laser pulse hits the surface in the normal direction, and that the surface is flat with good radiometric properties.

Soudarissanane (2016) points out that the quality of the laser scanner measurements is influenced by the following factors:

A. Scanner hardware (calibration, misalignment of components, detection methods, variation of the laser beam).
B. Atmospheric conditions (temperature, humidity, rain, air pressure, light conditions).
C. Scanning geometry.
D. Surface properties of the object.

Figure 6 illustrates these potential error sources. The scanner hardware (A) can introduce errors, originating from misalignment of components, echo detection method, time measurement method, or variation of the laser beam. Atmospheric conditions (B), such as temperature, humidity, rain, air pressure and light conditions, can cause errors. Some laser scanners are possible to calibrate to the actual temperature and air pressure. Fog, rain and snow can introduce “phantom points” by reflecting so much of the signal that false points are detected. The scanning geometry (C) can introduce systematic errors if the distance to the scanner varies within the footprint. This error source depends on the angle of incidence. A low angle of incidence gives a more stretched footprint, and the possible error is larger than when the angle of incidence is orthogonal to the object. A bias to shorter measurements when the angle is low follows. For tree stem measurements, this results in overestimated diameters, because the points on the “flanks” of the trees will be placed outside the stem. Lastly, the surface properties (D) of the object can cause errors. A shiny object reflects more photons back to the scanner and gives a stronger echo signal with a steeper leading edge than a diffuse object. Then, the echo will be detected earlier and a shorter distance is measured. When two objects, (C+D), reflect the same pulse, either two different points, one correct point from one of the objects, or a false point between the objects can be recorded.

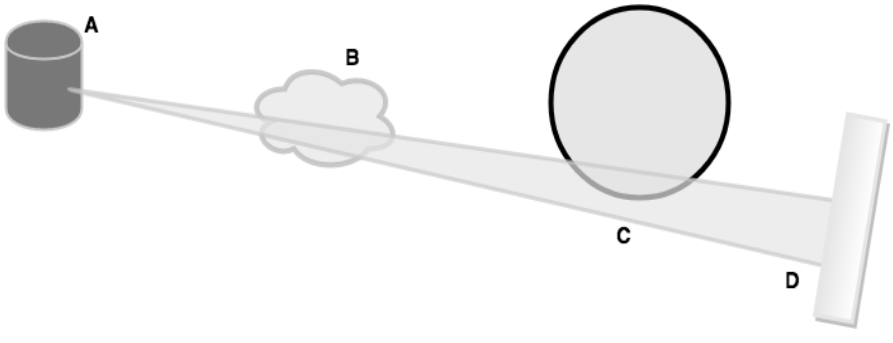

Figure 6. Possible error sources in laser scanning are (A) scanner hardware, (B) atmospheric conditions, (C) scanning geometry such as a sloped or curved surface, and (D) surface properties, such as a highly reflective surface. Multiple targets (C+D) can introduce false points.

1.6 Point cloud processing

1.6.1 Co-registration

Whether using images or laser scanning, if a larger point cloud is needed than a single view offers, multiple point clouds have to be co-registered. For co-registration of a set of point clouds, a rigid body transformation needs to be found to place them in the same coordinate system. A minimum of three matching points between the coordinate systems is required to find the transformation matrix. Depending on the source of the point cloud, different methods can be used.

1.6.2 Photogrammetric point clouds

For photogrammetric point clouds, matching points between the views can be detected, and used as source to find the rigid body transformation. Another possible approach is to extract matching shapes from the point clouds, and find the required transformation to put them in the same point cloud.

1.6.3 TLS point clouds

There are two distinctive approaches for co-registration of TLS point clouds, with or without artificial markers. One way to use artificial markers is to set up extra tripods for scanner placement before the first scanning. On each tripod, an artificial marker is placed, often a reflective sphere that is easy to detect in the point cloud. The scanner is then moved to another of the tripods for the next scanning, and so on. Then the scanner position and orientation for each scanning is easy to determine using the spheres, which are distinctive and easy to detect in the point clouds. Without artificial markers, the different point clouds have to be aligned to each other, using either manually detected features or automatic algorithms. A co-registered TLS point cloud is called *multiple-view* TLS, as opposed to *single-view TLS*, where only the point cloud from one scanner position is used, and *multiple single-view* TLS, where the results from multiple scanner positions are aggregated into tree maps.

1.6.4 Mobile Laser Scanning

A common approach for mobile laser scanning (MLS) is to use a moving laser scanner, scanning in one or multiple planes. The scanner position and direction are recorded for each scan using combinations of GNSS (Global Navigation Satellite System), IMU (Inertial Measurement Unit) and SLAM (Simultaneous

Localization and Mapping; Nüchter et al. 2007) localization from video camera images or laser data. Using the scanner position and direction for each plane, the points in the plane can be transformed into a point cloud with all the recorded points. Very high precision is required in the positioning to make a point cloud of high quality.

1.6.5 Workflow for tree stem attribute estimation

Four main functions are needed in a method for tree stem diameter estimation (Olofsson et al. 2014). A common model for estimation of tree stem attributes, usually diameter at breast height and position, from a point cloud is as follows:

1 Segmentation of the point cloud.
2 Classification of tree stem points / ground points / other points / noise.
3 Calculation of a ground model.
4 Estimation of diameter (at breast height, or at multiple heights for a stem profile) and tree position.

1.6.6 Methods for diameter estimation

There are many possible ways to estimate the stem diameter from a set of points. The choice of method to use in a specific setting depends mostly on the risk for outliers, noise in the point cloud, and the computational cost.

Angular methods calculate the stem diameter based on the angle between the outermost points on the stem, and the distance to either the closest point, and/or the outermost points. These methods are computationally cheap, but they are sensitive to errors in the segmentation and position errors in the few points that are used. The Two-Triangle method and the Viewing-Angle method are two examples of angular methods (Bailey & Nebot 2001; Selkäinaho 2002; Ringdahl et al. 2013).

Circle fit methods from a single view can perform well to create good diameter estimates, if the tree is actually circular. However, a slight ellipsoid shape is common, and the difference between the “thin” and the “wide” diameter are observed to be in the order of 5%. To minimize this problem manual caliper measurements are often made crosswise, and the mean is used as the stem diameter to avoid this problem. The circle fit methods are sensitive to noise. A good segmentation and outlier removal are important for good results. Also, point bias from the scanning geometry can influence the error significantly. There are many algorithms for circle fit, such as RANSAC (Fischler & Bolles 1981), algebraic fit and geometric fit (Gander et al. 1994; Nocedal & Wright 2006), among others. A cylinder fit or cone fit, where points from a longer

section of the stem is used, reduces the noise sensitivity and makes a diameter estimation possible even if the point cloud near the breast height area is noisy or occluded (de Conto et al. 2017).

In single view point clouds, only one side of each tree is visible, and less than half the circumference will be covered by points. In these point clouds, the ellipticity of tree stems is a prominent error source. Also, the larger errors in the flank points are pivot points for the diameter estimation, and may influence the results to a large extent.

If a multiple-view point cloud is correctly co-registered from different single-view clouds, circle fit algorithms can provide good estimates, especially if points of low quality (low angle of incidence) are removed. This requires however a good co-registration process.

One alternative to the co-registration of the point clouds is to process them from their separate points of view, so called multiple single-view. Tree stems can be detected, measured and positioned in the different single-view point clouds, creating view-wise tree maps. Then, the tree maps can be co-registered using tree positions and/or known scanner positions to make a plot or stand map.

For MLS data, multiple approaches are used for diameter estimation. The large errors that often occur in the positioning of the laser scanner can introduce artefacts in the point cloud that make the common TLS-methods unsuitable. One approach is to detect stems in each scan-revolution, connect the detected stem parts into stems, and use the median value for diameters close to breast height as the DBH value.

1.7 Related works

The results from different studies of methods for estimation of tree stem diameters, tree positions, heights, and stem shapes are difficult to compare. Some methods have been evaluated on forest field plots, some on individual trees, some in park conditions, and some along a track through a forest stand. The stem density, size of the stems, the undergrowth and low-growing branches in a forest setting influences the result. Different aims of the studies result in different metrics of interest. Sometimes the tree positions were the main interest, sometimes DBH, tree height, stem shape or a combination thereof. In some studies the results for measurements of individual trees are not reported, and only plot or stand wise estimates of wood volume or biomass are presented. In this section, an overview of the literature on the research topic is presented.

1.7.1 Photogrammetry

The development of terrestrial photogrammetry for forest measurements has accelerated since the development of digital cameras. Using analogue images was found to not be feasible due to time-consuming manual measurements (Reidelstürz 1997).

Automatic identification of stems in images was presented by Fürst & Nepveu (2006). The software eCognition was used for the image processing. The results show that the diameter error increases with the height of the measurement position. Only a small sample of trees was used, and the authors did not seem satisfied with the results. The diameter estimation bias was 2.1% at 1 meter height and 4% at 2 meter.

Dick et al. (2010) positioned trees using panorama images of field plots where synthetic targets of known size were attached to the stems. The position accuracy was 0.40 ± 0.42 m, and 85% of the trees were within 0.5 m of the field measured position.

Forsman et al. (2012) presented a multi-camera rig equipped with five cameras, which was used to estimate DBH of single trees. In Forsman et al. (2016a) the multi-camera rig was used for a field plot inventory. Images were acquired in twelve directions from one point in the centre of the field plot. Overall, 76% of the trees on six field plots within 10 meters were successfully positioned. The diameter could be estimated for 40% of the trees with an RMSE of 2.8—9.5 cm. Problem with the lighting conditions reduced the useful data set.

Liang et al. (2014b) was the first photogrammetric study evaluated on a forest field plot. An uncalibrated hand-held camera was used on a 30 m × 30 m forest field plot using a set of different image acquisition schemes. An outside path around the plot produced the best results, with a mapping accuracy of 88%, and RMSE of DBH was 2.39 cm.

Berveglieri et al. (2014) used vertical fisheye images for estimation of tree positions and DBH. The technique was tested in two urban forest areas with an RMSE of 1.8 cm and standard deviation 0.7 cm. In Berveglieri et al. (2016), vertical fisheye images from multiple heights were used for stem diameter estimation. For seven trees within 10 meters from the camera setup, DBH were estimated with an average error of 1.46 cm, and standard deviation 1.09 cm. In Berveglieri et al. (2017), the fisheye results were compared to terrestrial laser scanning using cylinder fit of presumed tree stems. The average difference between the cylinders from the point cloud was less than 1 cm. The point density of the optical cloud (from the fisheye images) was one-third that of the laser scanner cloud.

Rodríguez-García et al. (2014) used stereoscopic hemispherical images from a single point of view for estimation of the DBH of 30 trees in a Eucalyptus plot.

An error of 0.15 m in the distance to the tree was reported, together with an RMSE of the DBH of 1.51 cm (10.43%). The tree position RMSE was 0.23 m (8.95%).

Fritz et al. (2013) surveyed a forest stand with an open canopy using SfM (Structure from Motion; Hartley & Zisserman 2003, Westoby et al. 2012) and imagery from a UAV (Unmanned Aerial Vehicle). The point cloud was compared to a point cloud from terrestrial laser scanning of the forest stand. The camera angle from the UAV was 45 degrees, giving side-view images of the tree stems. The stem diameters were estimated using a RANSAC based cylinder fit on 50 cm thick slices of clusters assumed to be stems. Overall, 71% of the trees in the stand were possible to reconstruct. The diameters had a trend of being underestimated, but the performance using the TLS and the UAV data sets were similar.

Morgenroth & Gomez (2014) used SfM-MVS (Structure from Motion with Multiple View Stereophotogrammetry) from uncalibrated cameras to create point clouds of single trees. The method was tested on three trees, and gave 2.59% error for tree height estimates and 3.7% error in stem diameter estimates. They reported problems with the method in shadowed areas.

Fang & Strimbu (2017) used a Structure from Motion method. They found that the lighting and background conditions were significant for the point cloud quality. Less than 2 minutes per tree for fieldwork (15 min/500 m^2 plot) were needed. Eighteen trees were surveyed, with successful reconstruction of the trunks at up to 12 m height of all trees. Diameter estimates were done in AutoCad using side-view measurements respectively measurement of the convex hull. The result of DBH measurements was a bias of 12 mm (3.0%) and RMSE of 17.1 mm (5.6%).

Hyyppä et al. (2017) demonstrated the feasibility of the Microsoft Kinect and Google Tango sensors for forest measurements. With the Kinect sensor DBH was estimated with an RMSE of 1.90 cm. With Tango the bias was 0.3 cm and RMSE 0.73 cm compared to tape-measured DBH. The tree stem could be measured for lower parts of trees. The trees were individually measured with the sensor moving around each single tree.

Mokroš et al. (2018) compared seven different methods for producing a dense point cloud. The methods used combinations of different camera orientations, mobile capturing or stop-and-go, different holding methods, and different paths over the plot. The tree detection rate was 49—81% for the different paths and DBH was estimated with RMSE of 4.41—5.98 cm. The best result was achieved using a vertical camera orientation, stop-and-go shooting mode, and a path leading around the plot with two diagonal paths through the plot.

Campos et al. (2018) introduces a low-cost Personal Mobile Terrestrial System (PMTS) approach comprising an omnidirectional camera with off-the-shelf navigation systems and its evaluation in a forest environment. Point cloud quality accuracy was consistent with a ground sampling distance of 3.5—7 cm. Tree positions were measured with errors within 3.5—7 cm. Stem diameters were not measured.

1.7.2 TLS

Terrestrial laser scanning for forest measurements is operational on a small-scale, with some companies offering TLS based forest inventory. There is a lot of research done using TLS for various forest measurements, and in this section a few examples are presented.

The development of methods for estimation of tree stem attributes using TLS began about 15 years ago. Single trees were modelled by Pfeifer et al. (2004) and plotwise studies were done by Thies et al. (2004). Many methods have been developed since then, and the results are promising for plot inventory. On four different plots, Maas et al. (2008) estimated DBH with RMSE of 1.8—3.3 cm and bias of -0.7—1.6 cm.

Olofsson et al. (2014) achieved an RMSE of 14% (RMSE 2.0—4.2 cm, bias 0.6 cm) using a method combining a Hough transform and RANSAC for tree detection and diameter estimation. The method was validated on 16 field plots with a radius of 20 m using a single scan setup.

Liang et al. (2014c) determined stem curves using a TLS multiscan setup, with an accuracy of ~1 cm, for a set of 28 trees that were cut down and diameters were measured with a caliper.

Brolly & Király (2009) used three different methods, one single circle fit (RMSE 4.2 cm, bias -0.8 cm), one multiple circle fit (RMSE 3.4 cm, bias -1.6 cm) and one cylinder fit method (RMSE 7.0 cm, bias 0.5 cm). Liang et al. (2016) have in an overview of the field compared a number of works estimating the DBH. The best method performed DBH estimations with an RMSE of 0.7—2.4 cm, with bias -0.2—0.8 cm.

Lindberg et al. (2012) estimated DBH with an RMSE of 38.0 mm (13.1%) and bias of 1.6 mm (0.5%) with a method validated on six 80 m × 80 m plots. The results were used as training data for an ALS method.

The above-ground biomass can be estimated from measured stem profiles. Hauglin et al. (2013) have used TLS derived features to estimate the biomass of tree branches. Models for estimation of the total biomass above ground have been developed by Kankare et al. (2013). The stem curve and the crown size was used as model parameters. Hackenberg et al. (2015) have not

estimated the wood biomass, but the biomass of the leaf foliage, which is of interest regarding carbon absorption.

1.7.3 MLS

The wide range of results that are reported for estimations of DBH from MLS are complicated to compare due to different metrics and different methods for evaluation. With an early system described by Jutila et al. (2007) and Öhman et al. (2008) DBH was estimated with an average error of 4% for 72 measurable trees out of 277 observed trees. Outdoor environments were reconstructed by Fentanes et al. (2011) using a robot equipped with a rotating line-laser scanner. Hellström et al. (2012) used a 2D laser scanner mounted on a forest harvester. The DBH was estimated for 19 trees using six different methods with large mean errors, 53—87%. The precision of a set of diameter estimation methods was evaluated in a controlled environment with a line laser scanner by Ringdahl et al. (2013). They managed to reduce the error of the best method to 12%.

Circle fit with very small errors, 4.29 mm, has been achieved by Dian et al. (2011). However, their reference data was measurements in the point cloud without accounting for the physical error of the laser measurements. Basal area has been derived by Brunner & Gizachew (2014) with errors of around 10 m^2/ha for individual scans. A high-end 3D laser scanner was mounted on an ATV by Liang et al. (2014a). A mapping accuracy of 87.5% with an RMSE of DBH of 2.36 cm was achieved.

In a laboratory setting, the radius of tree trunks has been estimated with a relative bias of 4% by Kong et al. (2015) by using multiple stationary scans at the same height to reduce the influence of statistical errors in the distance measurement. Kelbe et al. (2015) retrieved stem locations with RMSE 0.16 m and DBH with an RMSE of 6 cm using a low resolution 2D laser scanner.

In Bauwens et al. (2016), an approach using a hand-held laser scanner is compared to a TLS single scan and a multiscan method. The hand-held laser scanner gave the best DBH results with bias of -0.08 cm and an RMSE of 1.11 cm. In Forsman et al. (2016), DBH were estimated with bias 2.3% and RMSE 14%.

1.7.4 Studies of error sources

There are many calculations involved in the process of deriving forest variables from terrestrial point cloud data and the results can be disturbed or biased due to many reasons. Point measurement errors due to sloped terrain in aerial laser

scanning is described by Schaer et al. (2007), Toth (2009), and in long range TLS by Fey & Wichmann (2017). Similar effects as temporal spreading of the pulse from sloped or stepped surfaces are noted by Jutzi & Stilla (2003) and the limitations in detail resolution are studied by Pesci et al. (2011).

The influence of the TLS scan mode on circle fitting is studied by Pueschel et al. (2013). Forsman et al. (2018) studied by simulation the errors in stem diameter estimations caused by scanner beam width, distance, and stem diameter. Krooks et al. (2013) have studied the intensity incidence angle effect, which can cause errors in the point measurements. In Soudarissanane (2016) the geometric error sources are evaluated in detail. Further knowledge about the object scanner geometry are used by Kelbe et al. (2015, 2016) to reduce the often impractical calculation load when using terrestrial point clouds containing millions of 3D points.

2 Objective of the thesis

The overall aim of this thesis is to develop and evaluate automatic methods for tree stem diameter estimation using ground-based sensors, such as cameras and laser scanners. A secondary aim is analysis of error sources to improve the understanding of the quality of the estimated variables.

The specific objectives of Papers I-IV were

I to develop methods and test the feasibility of terrestrial stereo-photogrammetry using a multi-camera rig for stem diameter estimation in hemi-boreal forests.

II to improve the diameter estimates and reduce the errors by treating the data line-wise for a data set from mobile laser scanning.

III to investigate errors related to the beam width effect on diameter estimation of cylindrical object.

IV to investigate whether a combination of distance and intensity panorama images from a terrestrial laser scanner could be used to accurately identify tree stem points in a point cloud.

3 Materials and methods

3.1 Paper I: Estimation of Tree Stem Attributes Using Terrestrial Photogrammetry with a Camera Rig

3.1.1 Materials

Field data were acquired at Remningstorp estate (N58.46°, E13.65°) in southern Sweden during August 2011. Reference data were collected using digital calipers for DBH measurement and total station for positioning. The field plots were also scanned with a terrestrial laser scanner.

A triangular camera rig equipped with a baseline of 114 cm and height of 36 cm was designed to 1) give the possibility of crosswise constrained epipolar matching of feature points, and 2) reduce the problems with occlusions. Three of the cameras were Canon EOS 7D with Sigma lenses. Two older Canon 40D cameras with zoom lenses were also added to the rig. The single cameras and the whole rig were calibrated using the PhotoModeler calibration pattern, to assess the internal camera parameters and the rig geometry (external parameters).

Due to difficult lighting conditions (strong sunlight and dark shadows), only six of the field plots were suitable for processing. The protocol required imagery in twelve directions, and if a single view was impossible to co-register to the point cloud, the plot had to be discarded. The older cameras were found to have issues with optical stability, and those images were only used in certain circumstances.

3.1.2 Method

In this study, a process for the photogrammetric process of estimating tree stem diameters and positions on field plots adapted to the triangular camera rig was

implemented. For camera- and rig calibration, the code developed by Börlin & Grussenmeyer (2013, 2014) was used.

The image processing pipeline requires a low level of operator interaction. The input data to the pipeline consist of images from one field plot and calibration images. Scale Invariant Feature Transform (SIFT, Lowe 2004) was used to detect feature points in the images. Cross-wise epipolar constraints were used to reduce the matching space, and for improvement of the matching quality. From the images, a point cloud was calculated for each view and co-registered using points visible in both clouds into a point cloud for the whole field plot. The point cloud was segmented using the algorithm by Rabbani et al. (2006). A ground model was calculated from the ground segments. The stem segments were verticalized using Principal Component Analysis. A cylinder with a height of one meter centred at 1.3 m was cut from each segment and projected into 2D. Diameters were estimated using algebraic circle fit (Gander et al. 1994). From the stem segments, the DBH was estimated by circle fitting to a 2D projection of the points closest to breast height (1.3 m).

3.2 Paper II: Tree Stem Diameter Estimation from Mobile Laser Scanning Using Line-Wise Intensity-Based Clustering

3.2.1 Materials

Mobile laser scanner data were acquired in Östergötland at the Sonstorp, Malmköping and Älvan test areas. Reference data were collected on 20 m × 20 m field plots along forest tracks. These data were collected for an earlier project (Barth et al. 2012). Stem diameters were measured using a digital caliper, and the trees were positioned using ultrasonic trilateration in relation to the field plot center.

A SICK LMS511 laser scanner was mounted on a roof rack on an off-road vehicle. The scanner was mounted forward-facing and angled 9° downward from a horizontal plane. The Chameleon positioning system (Rydell and Emilsson 2012), originally developed by FOI (Swedish Defence Research Agency) for tracking a person in GNSS-denied environments, was used for recording the trajectory. The Chameleon system consists of an Xsens MTi-G IMU (Xsens Technologies) and a Point Grey Bumblebee XB3 (FLIR Integrated Imaging Solutions) stereo camera. The movement recorded by the IMU is fused with the calculated movement from visual SLAM on the image stream to reduce the drift of the system. Point clouds from a mobile laser scanner traced with this system

will include some artefacts, such as trees split in two, or height discontinuities in the cloud.

3.2.2 Method

The scan lines from the 2D laser scanner were co-registered using the position and rotation data from the Chameleon system; however, the position and rotation data included a lot of noise. The resulting point cloud had a lot of artefacts, for example, stems were cut into two pieces, and shifted from each other. These irregularities made the point cloud unsuitable for normal point cloud techniques, such as cylinder detection, or 2D projection of a section of the stem for diameter estimation. Hence, the data were treated as lines and not a point cloud. Possible tree segments were detected by peak detection in the distance data, and segments close to each other were connected into trees. The geometrical endpoints of the segments were found to be biased in the distance measurement — they were too close to the scanner — and also had low intensity values. Therefore, points with low intensity were removed.

The stem diameter was estimated using four different methods. Three of the methods used a line-wise approach, where the stem diameter was estimated using the line segments close to breast height of each tree. The methods used different approaches; a circle fit and two different trigonometric techniques. The stem diameter was then determined, for each tree and method, as the median value of the line-wise estimated diameters. The fourth method projected the segmented points from multiple lines reflected by the tree onto a ground plane. The stem diameter was estimated using circle fit on the set of projected points.

3.3 Paper III: Bias of cylinder diameter estimation from ground-based laser scanners with different beam widths: A simulation study

3.3.1 Materials

This study is mainly a computer simulation study. For validation of the simulation, a physical reference laser scanning was performed using a SICK LMS 221. The scanned object was a cylindrical concrete pillar in the SLU (Swedish University of Agricultural Sciences) building in Umeå.

3.3.2 Method

A laser scanner simulator was implemented and used to evaluate various properties, such as distance, cylinder diameter, and beam width of a laser scanner-cylinder system to find critical conditions. The properties were chosen to imitate practical situations in laser scanning of forest, with beam width-angular separation combinations within the range of practically used laser scanners, tree diameters from 10—50 cm, and distances from 5—20 m. The laser beam was discretized into rays. For each ray, the intensity was calculated from a normal distribution. The travel time from the scanner to the object and back was calculated, and the dampening from reflection on the diffuse cylinder surface was also calculated. The signal (intensity depending on time) returning to the laser scanner was calculated by addition of the ray values. A distance value was calculated using a computed detection threshold in the signal. Laser points were simulated horizontally over the object, and diameter was calculated from the points.

3.4 Paper IV: Tree detection using intensity-based panorama images from terrestrial laser point clouds

3.4.1 Materials

This study was performed on an earlier collected TLS point cloud from Flakaträsk (N64.27°, E18.50°) in Northern Sweden. The forest is a dense, spruce dominated forest, with short lines of sight due to many branches and twigs. Many stems are partly occluded at 5 m distance, and very few are visible at 10 m. A Trimble TX8 laser scanner was used for the scanning. The reference data were collected for detailed evaluation of stem profiles on a few trees, and are unfortunately not sufficient for a full evaluation of this method. The results were instead compared with the results from another algorithm and with manual interpretation of the 3D data.

3.4.2 Method

Panorama images of the intensity and the distance values were constructed using the 3D coordinates and intensity values in the point cloud. The intensity image was classified using Fuzzy C-means clustering into 10 classes (Semechko 2013; Horváth 2006). Two of the classes included most of the tree stem pixels, and a small amount of other points. A binary image containing the stem pixels was constructed and segmented. The segments were connected using both closeness

in the binary image, and distance data to reject branches in front of the stem. The stem pixels were connected to the original 3D points, and the individual tree stems could be extracted from the point cloud.

4 Results and general discussion

4.1 Paper I: Estimation of Tree Stem Attributes Using Terrestrial Photogrammetry with a Camera Rig

As evidenced by several studies in the literature, photogrammetry in forests can be difficult due to difficult lighting conditions with many shadows. In this study, due to the lighting conditions and some faulty hardware, the imagery from only six out of 25 surveyed field plots were possible to use for making a point cloud of the whole plot. The method performed best on three plots with clearly visible stems with a 76% detection rate and 0% commission errors. Diameters could be estimated for 40% of the stems with an RMSE of 2.8—9.5 cm. The results are comparable to other camera-based methods evaluated in a similar manner (Liang et al. 2014b). The results are inferior to TLS-based methods, such as Liang et al. (2011) and Lindberg et al. (2012) among others.

For better imagery the images should be acquired in overcast but dry weather with good ambient lighting without shadows. The image acquisition from the center point of the plot, turning 30 degrees between images made the point cloud difficult to co-register with the chosen cameras. The overlapping part of the point cloud was small, and if one camera was occluded in that part, co-registration was almost impossible. A better planning of the image acquisition scheme, without the prerequisite of taking all images from one point for minimizing the time on the field plot, would be a straightforward way to reduce the co-registration problem, detect more trees on each field plot and improve the diameter estimates using points all around the circumference of the trees.

4.2 Paper II: Tree Stem Diameter Estimation from Mobile Laser Scanning Using Line-Wise Intensity-Based Clustering

In mobile laser scanning, the precision of the positioning of the laser scanner determines the quality of the co-registered point cloud. In this project, the point cloud was treated line-wise to reduce the effects from errors on the scanner positioning. Another observation from visual inspection of the line-wise stem segments was that the points did not follow a circle arc as was expected. The points on the ends of each line segment diverged from a circle indicated by the main part of the segment. It was found that the diverging points also had lower intensity values. An intensity filtering of the points was applied before diameter estimation to remove points that were assumed to have lower precision.

Algebraic circle fit on centred and 2D projected points was the most successful method, giving a relative bias of +2.3% and a relative RMSE of 14%. The median value of algebraic circle fit was more biased (+7%), but had a similar relative RMSE (15%). The Viewing Angle and the Two-Triangle methods made gross underestimations with relative bias of -29%, which was expected due to the removed low intensity points. The results are similar for all test areas, and no distinct conclusions can be made regarding the influence of various species or terrain (e.g., whether it is flat or sloped).

For comparison, a test was done using point clustering without the removal of low intensity points. All other parts of the code were identical. With this setup, the lowest performing methods (Viewing Angle and Two Triangle) gave slightly better results, and the best performing methods (Circle fit, Circle fit on 2D projection) gave much worse results with large positive bias. Keeping the intensity criterion and using Circle fit on 2D projected points gave the best results overall.

4.3 Paper III: Bias of cylinder diameter estimation from ground-based laser scanners with different beam widths: A simulation study

This study was initiated from the observation in Paper II that the points on the end of each stem segment, originating from the sides of the trees not facing the scanner, diverged from the presumed circle arc and influenced the diameter estimates to have a positive bias. The positive bias would influence the wood volume estimates made from the measured sample of trees.

The simulation results confirm that a positive bias of the diameter estimation was expected, and that a wider beam results in a larger error. For scanner parameters corresponding to a high-end TLS (i.e., beam width 0.02° and angular separation 0.01°) the resulting bias is small. In the worst case, a cylinder with a diameter of 5 cm scanned at 20 m gave a relative error of 2%. However, for scanners used for mobile laser scanning with wider beams, the error is larger, and for the two worst setups (beam width 0.63° with angular separation 0.33°, and beam width 0.8° with angular separation 0.25°) the relative error exceeded 10% for all test cases.

Large angular separation results in fluctuating error levels, due to a dependency on how far out on the stem side the outermost points are. By using a narrow angular separation (0.01°) for all beam widths, the beam width effect could be isolated. It was found that the bias followed a quadratic function of one parameter — the relative footprint, i.e., the fraction of the cylinder width illuminated by the laser beam. The quadratic function opened up the possibility to construct a compensation model for the bias.

4.4 Paper IV: Tree detection using intensity-based panorama images from terrestrial laser point clouds

The method presented in this paper detects trees in TLS point clouds in a computationally effective way, which reduces the time and cost required for the point cloud processing. For the detected trees the stem diameters can then be estimated using more conventional 3D methods with the improvement that only the interesting parts of the point cloud have to be processed.

In panorama image representation of a point cloud, the method detected trees that were wider than approximately 40 pixels (corresponding to 40 laser points in width reflected by a stem), and were within 5 meters of the scanner. The stem positions were similar to those detected using the method by Olofsson and Holmgren (2016). Stems close to each other were correctly detected as separate stems. A single birch tree was omitted, possibly because it was too curved to be accepted.

5 Conclusions

A ground-based method should be used under the same conditions for which it was developed. Methods developed for forests that are easy to model based on sensor data, such as sparse pine forests with low undergrowth, or park-like conditions, are probably not suitable test sites for more difficult conditions. Dense forests with tall undergrowth, or spruce trees with a lot of twigs, or irregularly shaped trees will probably cause gross errors, unless methods for handling these conditions are implemented.

Often, new methods are evaluated in easy conditions, such as in a sparse pine forest, or in park-like conditions with clearly visible stems. Successful results in such conditions do not make the method viable where more complicated conditions occur, such as where shrubs, undergrowth and twigs makes the ground level hard to determine, and the stem more difficult to delineate.

Point clouds from terrestrial photogrammetry, terrestrial laser scanning, and mobile laser scanning have different characteristics due to the different unique properties of the sensors. For successful estimation of forest variables, these properties have to be considered, both for planning of the data acquisition and for processing of the data. The point clouds can have different characteristics regarding, for example, density of the point cloud, distribution of errors in the point coordinates, errors introduced by co-registration, and auxiliary data such as point intensity or images. Understanding of these characteristics, especially how point errors appear, are important to accurately evaluate estimations based on the point cloud. There is a trade-off between the accuracy of the DBH measurement, and the amount of omission errors.

The knowledge about the sensor and the point cloud characteristics can also be used to simplify or improve the estimation of forest variables, resulting in faster calculations and higher quality of the results.

When the results are aggregated to plot or stand level statistics, such as basal area or wood volume, overestimations of DBH on single tree level can be

cancelled out by missing trees that were invisible from the scanner's point of view. A low bias can be achieved for the aggregated result, which can give a false impression of a trustworthy method. Therefore, tree-level validation should always be regarded as a necessary component when evaluating ground-based methods for estimation of forest variables.

References

Angel, E. (2009). *Interactive Computer Graphics: A Top-Down Approach Using OpenGL*. 5th ed. Pearson Education, Inc.

Bailey, T., and Nebot, E. (2001). Localisation in Large-Scale Environments. *Robotics and Autonomous Systems*. Vol. 37(4), pp. 261–81.

Baltsavias, E. P. (1999). Airborne Laser Scanning: Basic Relations and Formulas. *ISPRS Journal of Photogrammetry and Remote Sensing.* Vol. 54 (2), pp. 199–214.

Barth, A., Sonesson,J., Larsson, H., Engström, P., Rydell, J., Holmgren, J., Olofsson, K., Forsman, M. & Thor, M. (2012). *Beståndsmätning med mobila sensorer i skogsbruket*, Skogforsk. Available at: http://www.skogforsk.se/contentassets/5a178ef1764d4be5a371d0c4ccaeb18c/ arbetsrapport-773-bestandsmatning-med-olika-mobila-sensorer-i-skogsbruket.pdf.

Bauwens, S., Bartholomeus, H., Calders, K. & Lejeune, P. (2016). Forest Inventory with Terrestrial LiDAR: A Comparison of Static and Hand-Held Mobile Laser Scanning. *Forests*, vol. 7(6), 127.

Berveglieri, A., Oliveira, R.A. & Tommaselli, A.M.G., (2014). A feasibility study on the measurement of tree trunks in forests using multi-scale vertical images. In *The International Archives of the Photogrammetry, Remote Sensing and Spatial Information Sciences, Volume XL-5*.

Berveglieri, A., Tommaselli, A., Liang, X. & Honkavaara, E. (2016). Photogrammetric Measurement of Tree Stems from Vertical Fisheye Images. *Scandinavian Journal of Forest Research*, vol. 32(8). pp: 737-747.

Berveglieri, A., Tommaselli, A., Liang, X. & Honkavaara, E. (2017). Vertical Optical Scanning with Panoramic Vision for Tree Trunk Reconstruction. *Sensors*, vol. 17(12), 2791. Available at: http://dx.doi.org/10.3390/s17122791

Brolly, G. and Király, G. (2009). Algorithms for stem mapping by means of terrestrial laser scanning. *Acta Silvatica et Lignaria Hungarica*, vol. 5, pp: 119–130.

Brown, D.C. (1971). Close-range camera calibration. *Photogrammetric Engineering and Remote Sensing*, vol. 37(8), pp. 855–866.

Brunner, A. and Gizachew, B. (2014). Rapid detection of stand density, tree positions, and tree diameter with a 2D terrestrial laser scanner. *European journal of forest research*, vol. 133(5), pp. 819–831.

Börlin, N. and Grussenmeyer, P. (2013) Bundle Adjustment with and without Damping, *Photogrammetric Records*, vol 28 (114), pp: 396-415.

Börlin, N. and Grussenmeyer, P. (2014) Camera Calibration using the Damped Bundle Adjustment Toolbox. *ISPRS Annals of the Photogrammetry, Remote Sensing and Spatial Information Sciences*, vol II (5), pp. 89-96.

Campos, M.B, Tommaselli, A.M.G., Honkavaara, E., Prol, F.S., Kaartinen, H, El Issaoui, A. & Hakala, T. (2018). A Backpack-Mounted Omnidirectional Camera with Off-the-Shelf Navigation Sensors for Mobile Terrestrial Mapping: Development and Forest Application. *Sensors*, vol. 18(3), 827. Available at: http://dx.doi.org/10.3390/s18030827.

de Conto, T., Olofsson, K., Görgens, E.B, Rodriguez, L.C.E & Almeida, G. (2017). Performance of stem denoising and stem modelling algorithms on single tree point clouds from terrestrial laser scanning. *Computers and Electronics in Agriculture*, vol. 143, pp. 165–176.

Dai, F., Feng, Y. & Hough, R. (2014). Photogrammetric Error Sources and Impacts on Modeling and Surveying in Construction Engineering Applications. *Visualization in Engineering*, vol. 2(1).

Dian, W., Jinhao, L. & Jianli, W. (2011). Diameter fitting by least square algorithm based on the data acquired with a 2-D laser scanner. *Procedia Engineering*, vol. 15, pp. 1560-1564.

Dick, A.R., Kershaw, J.A. & MacLean, D.A. 2010. Spatial Tree Mapping Using Photography. *Northern Journal of Applied Forestry*, vol. 27(2), pp: 68–74.

Duvemo, K. & Lämås, T. (2006). The Influence of Forest Data Quality on Planning Processes in Forestry. *Scandinavian Journal of Forest Research*, vol. 21 (4), pp. 327–339.

Fang, R. & Strimbu, B.M. (2017). Stem Measurements and Taper Modeling Using Photogrammetric Point Clouds. *Remote Sensing*, vol. 9(7), 716.

Fentanes, J.A.P, Alonso, R.F., Zalama, E. & Garcia-Bermejo, J.G. (2011). A new method for efficient three-dimensional reconstruction of outdoor environments using mobile robots. *Journal of Field Robotics*, vol. 28(6), pp. 832–853.

Fey, C. and Wichmann, V. 2017. Long-range terrestrial laser scanning for geomorphological change detection in alpine terrain – handling uncertainties. *Earth Surface Processes and Landforms*, vol. 42(5), pp. 789–802.

Fischler, M.A. and Bolles, R.C. (1981). Random Sample Consensus: A Paradigm for Model Fitting with Applications to Image Analysis and Automated Cartography. *Communications of the ACM*, vol. 24(6), pp. 381–395.

FLIR Machine Vision, Inc. (2018). "Bumblebee XB3 FireWire Stereo Vision Camera Systems." Accessed January 24, 2018. https://www.ptgrey.com/bumblebee-xb3-1394b-stereo-vision-camera-systems-2.

Forsman, M., Börlin, N. & Holmgren, J. (2012). *Estimation of Tree Stem Attributes Using Terrestrial Photogrammetry. In: International archives of photogrammetry and remote sensing.* XXIIX ISPRS Congress. Melbourne, Australia, Aug 25-Sep 1, 2012, pp, 261–265

Forsman, M., Borlin, N. & Holmgren, J. (2016a). Estimation of Tree Stem Attributes Using Terrestrial Photogrammetry with a Camera Rig. *Forests*, vol. 7(3), 61. Available at: http://dx.doi.org/10.3390/f7030061.

Forsman, M, Holmgren, J. & Olofsson, K., (2016b). Tree Stem Diameter Estimation from Mobile Laser Scanning Using Line-Wise Intensity-Based Clustering. *Forests*, vol. 7(9), 206. https://doi.org/10.3390/f7090206.

Forsman, M., Börlin, N., Olofsson, K., Reese, H. & Holmgren, J. (2018). Bias of cylinder diameter estimation from ground-based laser scanners with different beam widths: A simulation study. *ISPRS journal of photogrammetry and remote sensing*, vol. 135, pp. 84–92.

Fridman, J. (2016). *Inventory Design. Swedish University of Agricultural Sciences*. Available at: https://www.slu.se/en/centrumbildningar-och-projekt/riksskogstaxeringen/om-riksskogstaxeringen1/om-inventeringen/. [2018-02-11]

Fritz, A., Kattenborn, T. and Koch, B. (2013). *UAV-based photogrammetric point clouds - Tree stem mapping in open stands in comparison to terrestrial laser scanner point clouds. Int. Arch. Photogramm. Remote Sens. Spatial Inf. Sci.*, XL-1/W2, pp. 141-146, https://doi.org/10.5194/isprsarchives-XL-1-W2-141-2013

Fürst, C. and Nepveu, G., (2006). Assessment of the assortment potential of the growing stock – a photogrammetry based approach for an automatized grading of sample trees. *Annals of forest science*, vol. 63, pp: 951–960.

Gander, W., Golub, G. H. and Strebel, R. (1994). Least-Squares Fitting of Circles and Ellipses. *BIT. Numerical Mathematics*. Vol. 34 (4). pp: 558–578.

Hackenberg, J., Wassenberg, M., Spiecker, H. & Sun, D. (2015). Non Destructive Method for Biomass Prediction Combining TLS Derived Tree Volume and Wood Density. *Forests*, vol. 6(4), pp. 1274–1300.

Hauglin, M., Astrup, R., Gobakken, T. & Næsset, E. (2013). Estimating single-tree branch biomass of Norway spruce with terrestrial laser scanning using voxel-based and crown dimension features. *Scandinavian journal of forest research*, vol. 28(5), pp. 456–469.

Hartley, R. I. and Zisserman, A. (2003). *Multiple View Geometry in Computer Vision*. Cambridge University Press, ISBN: 978-0-521-54051-3.

Hellström, T., Hohnloser, P. & Ringdahl, O., (2012). *Tree diameter estimation using laser scanner*, Department of Computing Science. Available at: http://www8.cs.umu.se/research/uminf/reports/2012/020/part1.pdf.

Hirschmüller, H. (2008). Stereo Processing by Semiglobal Matching and Mutual Information. *In IEEE Transactions on Pattern Analysis and Machine Intelligence*, vol. 30 (2), pp. 328-341, doi:10.1109/TPAMI.2007.

Holopainen, M., Vastaranta, M., and Hyyppä, J. (2014). Outlook for the Next Generation's Precision Forestry in Finland. *Forests*, vol. 5(7). pp: 1682–94.

Horváth, J. (2006). Image Segmentation Using Fuzzy C-Means. In *Symposium on Applied Machine Intelligence*. Avaiable at: http://uni-obuda.hu/conferences/sami2006/JurajHorvath.pdf.

Hyyppä, J., Virtanen, J.P., Jaakkola, A., Yu, X., Hyyppä, H. & Liang, X. (2017). Feasibility of Google Tango and Kinect for Crowdsourcing Forestry Information. *Forests*, vol. 9(1), 6.

Jutila, J., Kannas, K. & Visala, A. (2007). *Tree Measurement in Forest by 2D Laser Scanning. Proceedings of the 2007 IEEE International Symposium on Computational Intelligence in Robotics and Automation.* Jacksonville, FL, USA, June 20-23, 2007

Jutzi, B. & Stilla, U., (2003*). Analysis of laser pulses for gaining surface features of urban objects*. In *Remote Sensing and Data Fusion over Urban Areas, 2003. 2nd GRSS/ISPRS Joint Workshop on*. IEEE, pp: 13–17.

Kankare, V. et al. (2013). Individual tree biomass estimation using terrestrial laser scanning. *ISPRS journal of photogrammetry and remote sensing*, vol. 75, pp. 64–75.

Kelbe, D., van Aardt, J., Romanczyk, P., van Leeuwen, M. & Cawse-Nicholson, K. (2016). Marker-free registration of forest terrestrial laser scanner data pairs with embedded confidence metrics. *IEEE transactions on geoscience and remote sensing*, vol. 54(7), pp: 4314–4330.

Kelbe, D., van Aardt, J., Romanczyk, P., van Leeuwen, M. & Cawse-Nicholson, K. (2015). Single-Scan Stem Reconstruction Using Low-Resolution Terrestrial Laser Scanner Data. *IEEE Journal of Selected Topics in Applied Earth Observations and Remote Sensing*, vol. 8(7), pp. 3414–3427.

Kong, J., Ding, X., Liu, J., Yan, L. & Wang, J. (2015). New Hybrid Algorithms for Estimating Tree Stem Diameters at Breast Height Using a Two Dimensional Terrestrial Laser Scanner. *Sensors*, vol. 15(7), pp: 15661–15683.

Krooks, A., Kaasalainen, S., Hakala, T. & Nevalainen, O. (2013). Correction of Intensity Incidence Angle Effect in Terrestrial Laser Scanning. *ISPRS Annals of Photogrammetry, Remote Sensing and Spatial Information Sciences*, vol. II-5/W2, pp: 145–150.

Liang, X., Litkey, P., Hyyppä, J., Kaartinen, H., Kukko, A. & Holopainen, M. (2011). Automatic Plot-Wise Tree Location Mapping Using Single-Scan Terrestrial Laser Scanning. *Photogramm. J. Finland.* vol. 22 (2) pp: 37–48.

Liang, X., Hyyppä, J., Kukko, A., Kaartinen, H., Jaakkola, A. and Yu, X. (2014a). The Use of a Mobile Laser Scanning System for Mapping Large Forest Plots. *IEEE Geoscience and Remote Sensing Letters*, vol. 11 (9). pp: 1504–1508.

Liang, X., Jaakkola, A., Wang, Y., Hyyppä, J., Honkavaara, E., Liu, J. & Kaartinen, H. (2014b). The Use of a Hand-Held Camera for Individual Tree 3D Mapping in Forest Sample Plots. *Remote Sensing*, vol. 6(7). pp: 6587-6603

Liang, X., Kankare, V., Yu, X., Hyyppä, J. and Holopainen, M. (2014c). Automated stem curve measurement using terrestrial laser scanning. *IEEE transactions on geoscience and remote sensing: a publication of the IEEE Geoscience and Remote Sensing Society*, vol. 52(3), pp: 1739–1748.

Liang, X., Kukko, A., Kaartinen, H., Hyyppä, J., Yu, X., Jaakkola, A. and Wang, Y. (2014d). Possibilities of a Personal Laser Scanning System for Forest Mapping and Ecosystem Services. *Sensors*, vol.14(1), pp: 1228-1248. doi:10.3390/s140101228.

Liang, X. et al. (2016). Terrestrial laser scanning in forest inventories. *ISPRS journal of photogrammetry and remote sensing*, vol. 115, pp. 63–77.

Lindberg, E., Holmgren, J., Olofsson, K. & Olsson, H. (2012). Estimation of stem attributes using a combination of terrestrial and airborne laser scanning. *European journal of forest research*, vol. 131(6), pp: 1917–1931.

Lowe, D.G. (2004). Distinctive Image Features from Scale-Invariant Keypoints. *International Journal of Computer Vision*, vol. 60 (2). pp: 91–110.

Maas, H-G, Bienert, A., Scheller, S. and Keane, E. (2008). Automatic Forest Inventory Parameter Determination from Terrestrial Laser Scanner Data. *International Journal of Remote Sensing*, vol. 29 (5). pp:1579–193.

Mikhail, E.M, Bethel, J.S. and McGlone, J.C. (2001) *Introduction to Modern Photogrammetry*, Wiley.

Mokroš, M. et al. (2018). Evaluation of Close-Range Photogrammetry Image Collection Methods for Estimating Tree Diameters. *ISPRS International Journal of Geo-Information*, vol. 7(3), 93.

Morgenroth, J. & Gomez, C. (2014). Assessment of tree structure using a 3D image analysis technique—A proof of concept. *Urban Forestry & Urban Greening*, vol. 13(1), pp: 198–203.

Næsset, E., (2007). Airborne laser scanning as a method in operational forest inventory: Status of accuracy assessments accomplished in Scandinavia. *Scandinavian journal of forest research*. vol. 22(5), pp: 433–442.

Näslund, M. (1947). *Funktioner och tabeller för kubering av stående träd*, Available at: https://pub.epsilon.slu.se/9900/1/medd_statens_skogsforskningsinst_036_03.pdf. [2018-02-02]

Nilsson, M., Nordkvist, K., Jonzén, J., Lindgren, N., Axensten, P., Wallerman, J. and Egberth, M. (2017). A Nationwide Forest Attribute Map of Sweden Predicted Using Airborne Laser Scanning Data and Field Data from the National Forest Inventory. *Remote Sensing of Environment*. vol. 194 (June). pp: 447–454.

Nocedal, J., and Wright, S.J. (2006). *Numerical Optimization*. 2nd ed. Springer-Verlag.

Nüchter, A, Lingemann, K., Hertzberg, J. and Surmann, H. (2007). 6D SLAM—3D Mapping Outdoor Environments. *Journal of Field Robotics*. vol. 24 (8-9). pp: 699–722.

Öhman, M., Miettinen, M., Kannas, K., Jutila, J., Visala, A. and Forsman, P. (2008). Tree Measurement and Simultaneous Localization and Mapping System for Forest Harvesters. In *Field and Service Robotics*. Springer Tracts in Advanced Robotics. Springer Berlin Heidelberg, pp. 369–378.

Olofsson, K. and Holmgren, J. (2016). Single Tree Stem Profile Detection Using Terrestrial Laser Scanner Data, Flatness Saliency Features and Curvature Properties. *Forests* 7 (9) 207.

Olofsson, K., Holmgren, J. and Olsson, H. (2014). Tree Stem and Height Measurements Using Terrestrial Laser Scanning and the RANSAC Algorithm. *Remote Sensing*, vol. 6 (5). pp: 4323–44.

Olofsson, K. and Olsson, H. (2017): Estimating tree stem density and diameter distribution in single-scan terrestrial laser measurements of field plots: a simulation study, *Scandinavian Journal of Forest Research*, vol. 32 DOI: 10.1080/02827581.2017.1368698

Pesci, A., Teza, G. & Bonali, E. (2011). Terrestrial Laser Scanner Resolution: Numerical Simulations and Experiments on Spatial Sampling Optimization. *Remote Sensing*, vol. 3(1), pp: 167–184.

Pfeifer, N, Gorte, B. and Winterhalder, D. (2004). Automatic Reconstruction of Single Trees from Terrestrial Laser Scanner Data. *International Archives of Photogrammetry, Remote Sensing, and Spatial Information Sciences* XXXV (B5). 2004, Istanbul, Turkey. pp: 114–119.

Pueschel, P., Newnham, G., Rock, G., Udelhoven, T., Werner, W. & Hill, J. (2013). The influence of scan mode and circle fitting on tree stem detection, stem diameter and volume extraction from terrestrial laser scans. *ISPRS journal of photogrammetry and remote sensing: official*

publication of the International Society for Photogrammetry and Remote Sensing, vol. 77, pp: 44–56.

Reidelstürz, P. (1997). *Forstliches Anwendungspotential der terrestrisch - analytischen Stereophotogrammetrie*. der Albert-Ludwigs-Universität Freiburg, Breisgau.

Ringdahl, O., Hohnloser, P., Hellström, T., Holmgren, J. and Lindroos, O. (2013). Enhanced Algorithms for Estimating Tree Trunk Diameter Using 2D Laser Scanner. *Remote Sensing*. vol 5(10), pp:4839-4856.

Rodríguez-García, C., Montes, F., Ruiz, F., Canellas, I. & Pita, P. (2014). Stem mapping and estimating standing volume from stereoscopic hemispherical images. *European journal of forest research*, vol. 133(5), pp: 895–904.

Rydell, J. and Emilsson, E. (2012). "CHAMELEON: Visual-Inertial Indoor Navigation." In *Position Location and Navigation Symposium (PLANS), 2012 IEEE/ION*, 541–546.

Schaer, P., Skaloud, J., Landtwing, S. & Legat, K. (2007). Accuracy estimation for laser point cloud including scanning geometry. In *Mobile Mapping Symposium 2007, Padova*. Available at: http://www.isprs.org/proceedings/XXXVI/5-C55/papers/schaer_philipp.pdf.

Selkäinaho, J. (2002). *Adaptive Autonomous Navigation of Mobile Robots in Unknown Environments*. Diss. Helsinki University of Technology.

Semechko, A. (2013). *Fast Segmentation of N-Dimensional Grayscale Images - File Exchange - MATLAB Central*. Available at: https://se.mathworks.com/matlabcentral/fileexchange/41967-fast-segmentation-of-n-dimensional-grayscale-images [2018-01-29]

Shan, J and Toth, C.K. (2009), *Topographic Laser Ranging and Scanning*, CRC Press (2009)

Soudarissanane, S.S. (2016). *The Geometry of Terrestrial Laser Scanning; Identification of Errors, Modeling and Mitigation of Scanning Geometry.* Diss: Delft University of Technology, Nederlands. Available at: http://repository.tudelft.nl/islandora/object/uuid:b7ae0bd3-23b8-4a8a-9b7d-5e494ebb54e5/?collection=research. [2018-01-21]

Strang, Gilbert. (2003). *Introduction to Linear Algebra*. 3rd ed. Wellesley-Cambridge.

Thies, M., Pfeifer, N., Winterhalder, D. & Gorteb, B.G. (2004). Three-dimensional Reconstruction of Stems for Assessment of Taper, Sweep and Lean Based on Laser Scanning of Standing Trees. *Scandinavian journal of forest research / issued bimonthly by the Nordic Forest Research Cooperation Committee*, vol. 19(6), pp: 571–581.

Toth, C.K. (2009). Strip Adjustment and Registration. In J. Shan & C. K. Toth, eds. *Topographic Laser Ranging and Scanning Principles and Processing*. CRC Press, pp. 235–268.

Wagner W., Ullrich, A., Melzer, T., Briese, C., Kraus, K. (2004). From single-pulse to full-waveform airborne laser scanners: potential and practical challenges. *In: ISPRS Archives, vol. XXXV Part B3. ISPRS.*

Wikström, P., Edenius, L., Elfving, B., Eriksson, L.O., Lämås, T., Sonesson, J., Öhman, K., Wallerman, J., Waller, C., and Klintebäck, F. (2011). The Heureka Forestry Decision Support System: An Overview. *Mathematical and Computational Forestry & Natural Resource Sciences*, vol. 3(2), pp: 87-95.

Westoby, M.J., Brasington, J., Glasser, N.F, Hambrey, M.J., Reynolds, J.M. (2012) 'Structure-from-Motion' photogrammetry: A low-cost, effective tool for geoscience applications, *Geomorphology*, vol. 179, pp: 300-314. https://doi.org/10.1016/j.geomorph.2012.08.021.

Xsens Technologies (2018). “MTi-G (legacy Product) - Products - Xsens 3D Motion Tracking.” Xsens 3D Motion Tracking. Accessed January 24, 2018. https://www.xsens.com/products/mti-g/.

Popular science summary

There is a great demand for information about the forest state. At a global level, deforestation is monitored and biomass and bound carbon are estimated. National and regional authorities want to know, among other things, what assets are available, whether the forests are well managed, and what the recreational values of the forest are. Individual forest owners and forest owner's organizations need information to plan forest management, and also be able to value the forest. The information is collected with satellite and airborne remote sensing in combination with sample measurements of field plots. The size of the sample plots varies, but usually they are circles with a radius of 5—10 meters.

In field inventories, tree diameter at breast height (DBH, 1.3 m above ground) are measured with a caliper. It is a labor-intensive method that would need to be more efficient in order to obtain higher quality of the forest information. Ground-based sensors, such as laser scanners or cameras, could make the inventory faster, and larger samples could be inventoried. Harvester sensors could deliver tree maps of what remained after a harvest, or could collect data for a driver support system.

A laser scanner measures its surroundings by sending out pulses of laser light and measures the time until a light echo returns. The distance to the object reflecting the light is then calculated using the measured time. The laser scanner transmits the pulses systematically in different directions and record in which direction each echo comes from. With the distance and direction of an echo, the coordinate of a 3D point can be calculated. The echoes have different strengths, or intensities, depending on how the laser pulse hit the object, and the reflection properties of the object. All measurements together constitute a point cloud. Stationary terrestrial laser scanning (TLS) on field plots produce 3D measurements all around the scanner except at the spot where the scanner is placed. These laser scanners can measure a million points per second, and a typical scan takes 3 minutes. Mobile laser scanning (MLS) is usually done using line laser scanners, which measure the distances in one or a few planes. These

scanners are generally cheaper, and they have lower resolution and a wider laser beam. For the mobile laser scanning, one must keep track of the scanner's position carefully all the time in order to put the lines of laser points together into a point cloud.

Measurement using cameras is called photogrammetry. How the object is imaged in a camera can be calculated with a camera matrix. The camera matrix contains information about camera geometry, including focal length and sensor size, among other things. If you know the camera matrices for two images, and the relative orientation of the cameras (location and direction), you can calculate 3D coordinates for points identified in both images.

This thesis consists of four articles. The first article describes a photogrammetric method for estimation of stem diameter and position on sample areas. The sample areas were photographed from the field plot center in twelve directions with a camera rig equipped with five digital system cameras. For each direction, a point cloud was calculated, and these were assembled into one point cloud for the entire field plot. Problematic light conditions caused many images to be of low quality, and therefore only images from a few field plots were useful. On the useful field plots, 76% of the trees could be found and positioned, and on 40% the diameters could be estimated.

The second article is about mobile laser scanning. Laser data were collected in a previous project with a line laser scanner mounted on a car. The laser scanner pointed approximately 9 degrees downwards, and as the car moved, a point cloud was built over the area that had been passed through. The scanner position was derived using a system that combined data from a stereo-camera and an inertial measurement unit. The point cloud was then processed using a method that worked line-wise to find the trees and to estimate several individual diameters for each tree. In that way, errors resulting from the positioning system uncertainty could be reduced. In addition, it was found that the outermost points on each tree trunk were not located on the expected circle arc around the trunk. These points had lower intensity. By introducing an intensity condition in the delineation of the tree stems, these points could be avoided. Four different methods were tested to determine the stem diameter. The best method estimated the diameters with a mean error of only 2.3%. The third article examined why the points on the edges of the tree end up outside the expected arc by simulating laser scanners / tree combinations. The trees were simulated by cylinders that were 5-20 meters away from the laser scanner and had diameters of 10-50 cm. A variety of beam width and angle resolution combinations were tested, based on scanner data from different scanners used for tree measurements, both TLS and MLS. It turned out that a wider laser beam caused the diameter of a tree to be overestimated, because a point can be registered when only a fraction of the

beam is reflected. Thus, points representing the flanks of a stem appeared to have their positions in front of or even outside the stem. A relationship between the diameter error and the laser beam width relative to the stem diameter was found. Commonly used mobile laser scanners turned out to give a relative bias of 10% or more in the tested situations. The fourth article is about a method for automatic tree detection in TLS point cloud data for a sample plot using the intensity of the points. The point cloud was converted into a panoramic image where each pixel has the intensity value of the closest point measured in that direction. The points were then classified with an image analysis technique, and in that result the tree trunks were easy to find. When compared to a previously developed method, the new method was found to be better in separating closely-standing tree trunks, but the range was shorter. Only trees within about 5 meters were discovered, but there are opportunities to improve the method for a greater range.

The conclusions of the entire thesis are that point clouds from the different sensors (cameras, terrestrial laser scanning and mobile laser scanning) are useful for estimating tree diameters and positions, but they have sensor-dependent properties which can introduce errors. These characteristics, and the precision requirements should be considered when planning data collection and selecting a sensor. As sensors and methods develop further, their use will probably increase – making it increasingly important to know their strengths and weaknesses.

Populärvetenskaplig sammanfattning

Det finns stor efterfrågan på information om skogarnas tillstånd. På global nivå övervakas avskogning och görs skattningar av biomassa och bundet kol. Nationella och regionala myndigheter vill bland annat veta vilka tillgångar som finns, om skogarna förvaltas väl, och vilka rekreationella värden skogen har. Enskilda skogsägare och skogsägarorganisationer behöver information för att planera skogsskötseln, och även kunna värdera skogen. För att producera kartor används heltäckande fjärranalysdata från flyg- och satellitbaserade sensorer i kombination med stickprov från provytor för att skapa skattningsmodeller (funktioner). Storleken på provytorna varierar, men oftast är de cirklar med en radie på 5—10 meter.

Vid fältinventeringar mäts trädens diameter vid brösthöjd (DBH, 1.3 m) med klave. Det är en arbetsintensiv metod som skulle behöva effektiviseras för att få bättre kvalitet på den skogliga informationen. Markbaserade sensorer, som laserskannrar eller kameror, skulle kunna göra inventeringen snabbare och större stickprov skulle kunna inventeras. Sensorer på skördare skulle kunna leverera trädkartor över vad som är kvarlämnat efter en avverkning, eller de skulle kunna samla in data till ett förarstödsystem.

En laserskanner mäter upp sin omgivning genom att skicka ut pulser av laserljus och mäter tiden tills det kommer tillbaka ett ljuseko. Avståndet till det objekt som reflekterade ljuset beräknas sedan med hjälp av den uppmätta tiden. Laserskannern skickar pulserna systematiskt i olika riktningar, och registrerar i vilken riktning varje eko kommer ifrån. Med avståndet och riktningen för ett eko så kan en koordinat för en 3D-punkt beräknas. Ekot får olika styrka, eller intensitet, beroende på hur laserpulsen träffat objektet och hur det reflekterar laserljuset. Alla mätningarna tillsammans utgör ett punktmoln. För stillastående laserskanning (Terrestrial Laser Scanning, TLS), t.ex. av provytor, används 3D-laserskannrar som mäter runtom laserskannern utom en fläck rakt under den. Dessa laserskannrar kan mäta en miljon punkter i sekunden, och en typisk skanning kan ta 3 minuter. Till mobil laserskanning (MLS) används oftast

linjelaserskannrar, som mäter avstånden i ett eller några plan. Dessa är generellt billigare, och de har lägre upplösning samt bredare laserstråle. Till den mobila laserskanningen måste man hålla reda på skannerns position noggrant hela tiden för att kunna sätta ihop linjerna av laserpunkter till ett punktmoln.

Mätning med hjälp av kameror kallas för fotogrammetri. Hur objektet avbildas i en kamera kan beräknas med en kameramatris. Kameramatrisen innehåller information om kamerans geometri, bland annat brännvidd och sensorstorlek. Om man vet kameramatriserna för två bilder och kamerornas relativa orientering (plats och riktning) så kan man beräkna 3D-koordinater för punkter som identifierats i båda bilderna.

Denna avhandling består av fyra artiklar. Den första artikeln beskriver en fotogrammetrisk metod för skattning av stamdiameter och position på provytor. Provytorna fotograferades från deras mittpunkter i tolv riktningar med en kamerarigg utrustad med fem digitala systemkameror. För varje riktning beräknades ett punktmoln som sedan monterades ihop till punktmoln för hela ytan. Problematiska ljusförhållanden gjorde att många bilder hade för låg kvalité och därför var endast bilderna från ett fåtal provytor användbara. På de användbara provytorna kunde 76 % av träden hittas och placeras, och för 40 % kunde dessutom diametrarna skattas.

Den andra artikeln handlar om mobil laserskanning. Laserdata var insamlat inom ett tidigare projekt med en linjelaserskanner som var monterad på en bil. Laserskannern pekade ca 9 grader nedåt, och allt eftersom bilen rör sig byggs ett punktmoln upp över det område som passerats. Positionen registrerades med ett system som kombinerade positionering med SLAM (Simultaneous Localization And Mapping) med tröghetsnavigering. Punktmolnet behandlades sedan med en metod som arbetade linjevis med att hitta träden och skatta många enskilda diametrar för varje träd. På så vis kunde fel som kom från osäkerheten i positioneringssystemet minskas. Dessutom konstaterades det att de yttersta punkterna på varje trädstam inte hittades på den förväntade cirkelbågen runt stammen, utan låg utanför. Dessa punkter hade lägre intensitet. Genom att introducera ett intensitetsvillkor i avgränsningen av träden kunde dessa punkter undvikas. Fyra olika metoder testades för att bestämma stamdiameter. Den bästa metoden skattade diametrarna med ett bias på endast 2.3 %. I den tredje artikeln undersöktes varför punkterna på trädens kanter hamnar utanför den förväntade cirkelbågen genom simulering av laserskanner / trädkombinationer. Träden simulerades av cylindrar som stod på 5-20 meters avstånd från laserskannern och hade diametrar på 10-50 cm. Ett antal olika kombinationer av strålbredd och vinkelupplösning testades, som baserades på skannerdata från olika skannrar som använts för trädmätningar, både TLS och MLS. Det visade sig att en bredare laserstråle gör att diametern på ett träd överskattas, för att en punkt kan

registreras då endast en liten del av strålen reflekteras. Därför kan man få punkter som representerar stammens flanker, men ligger framför eller till och med utanför stammen. En relation mellan diameterfelet och laserstrålens bredd i förhållande till stamdiametern hittades. Vanligt använda mobila laserskannrar visade sig ge en relativ bias på 10 % eller mer i de testade situationerna.

Den fjärde artikeln handlar om en metod för att hitta trädstammar i ett TLS-punktmoln för en provyta genom att utnyttja punkternas intensitet. Punktmolnet användes för att beräkna en panoramabild där varje pixel har intensitetsvärdet för den närmaste punkt som mätts i den riktningen. Punkterna klassades sedan med en bildanalysteknik och i det resultatet syntes trädstammarna väl. Vid jämförelse med en tidigare TLS-metod visade det sig att den nya metoden vara bättre på att separera tätt stående trädstammar, men räckvidden var kortare. Endast träd inom ca 5 meter blev upptäckta, men det finns möjligheter att förbättra metoden till större räckvidd.

Slutsatserna för hela avhandlingen är att punktmoln från de olika sensorerna är användbara för uppskattning av stamdiametrar och positioner, men de har sensorberoende egenskaper som kan införa fel. Dessa egenskaper och precisionskravet bör beaktas när datainsamlingen planeras och sensorn väljs. Allteftersom sensorer och metoder utvecklas, så kommer de förmodligen att användas mer, vilket gör det viktigt att känna till deras styrkor och svagheter.

Acknowledgements

I would like to thank my supervisors for their time and engagement in my doctoral studies.

Tack till min huvudhandledare Johan för din tid och din entusiasm, för många idéer som bollats fram och tillbaka, och för att jag fått förtroendet att utforma så mycket av forskningen själv.

Till mina biträdande handledare vill jag säga:

Tack Niclas för att du tipsade mig om den här doktorandtjänsten, delat med dig av din tid även när den är slut, hjälpt till med kod, algoritmer och artiklar, gott kamratskap och för att du alltid tar dig tid att lyssna.

Tack Kenneth för långa och öppna diskussioner, oftast över en kopp kaffe, om allt från laserdata till science fiction.

Tack Heather för hjälp att styra arbetet åt rätt håll, och mycket hjälp med att göra min engelska läsbar. Lycka till i Göteborg!

Jag vill tacka Håkan Larsson, Phillip Engström och Joakim Rydell (FOI) och Andreas Barth (Skogforsk) för att jag fick vara med på en datainsamling med mobil laserscanner. Tack även till övriga delaktiga i "Mobila sensorer i skogsbruket"-projektet för att jag fått använda ert data.

Tack Ola Ringdahl för lån av en laserskanner och hjälp med denna.

Tack Thomas Hellström för opposition på mitt halvtidsseminarium och predisputation.

Tack Mats Nilsson för opposition på min predisputation.

Tack till Tommy Andersson för laserdata, och svar på praktiska frågor om laserskanning.

Stort tack till alla på avdelningen för fjärranalys. Ni är underbara och har varit ovärderliga! Tack Bisse, Ivan, Nils, Jörgen, Eva, Inka, Mats H, Mats N, Jonas

B, Jonas J, Karin, Emma, Henrik, Mattias, Peder, Micke, Arvid, André, Micke, Håkan, Frasse.

Tack till Nanna, Anne-Maj, Ylva och Carina för hjälp med allt möjligt administrativt.

Tack Hans och Gun för hjälp att hitta igenom den administrativa doktorand-labyrinten.

Och sen ett stort tack till alla på institutionen många trevliga och lärorika stunder över kaffekoppar och luncher! En fantastisk sak med att jobba på SRH är att man aldrig vet vad man råkar lära sig under lunchen. Några av alla som kan ta åt sig äran är: Mikaela, Cornelia, Per S, Karin Ö, Ylva M, Anders P, Johanna, Tomas L, Anna A, Helena, David A, Anna-Lena, Carola, Neil, Hans G, Jonas F, Anton G, Henrik H, Mikael H, Gun, Maud, Torgny, Dianne, Anders M, Pär N, Eva-Maria, Bo-Gunnar, Jonas D, Jocke, Anders S, Elias, Patrik U, Mats W, Per-Erik, Mats S, Erik W, Xin, Rami, Marianne, Julia, Sebastian, Miloutin, Mozhgan, och många andra.

Hej Mona! Tack för många skratt!

Sen måste jag tacka pappa Klas, mamma Runa, mina bröder Torbjörn och Anders - ni har lärt mig att det går att lära sig vad som helst. Har man inte försökt så vet man ju inte om man kan, så det är lika bra att testa!

Pappa, jag blev klar före dig!

Stort tack till min make Tomas, som varit till fantastiskt stöd, såväl med att bolla och ifrågasätta idéer, felsöka kod och kritiskt granska allt jag skriver, som att hålla familjen flytande och fixa allt när jag ägnat kvällarna åt att skriva.

Och till sist: Tack till mina underbara barn, Sixten och Olivia, som med enorm nyfikenhet och fantasi lyser upp tillvaron och ser till att jag har roligt!